The Kinetic Aspects of Intracellular Fluorescence Labeling with TMA-DPH Support the Maturation Model for Endocytosis in L929 Cells

Dominique Illinger and Jean-Georges Kuhry

Laboratoire de Biophysique, URA491 du Centre National de la Recherche Scientifique, Université Louis Pasteur, Strasbourg, France

Abstract. TMA-DPH (1-(4-trimethylammonium)-6-phenyl-1,3,5-hexatriene), a hydrophobic fluorescent membrane probe, interacts with living cells by instantaneous incorporation into the plasma membrane, where it becomes fluorescent. It then follows the intracellular constitutive membrane traffic and acts as a bulk membrane marker of the endocytic pathway (Illinger, D., P. Poindron, P. Fonteneau, M. Modolell, and J. G. Kuhry. 1990. *Biochim. Biophys. Acta.* 1030:73–81; Illinger, D., P. Poindron, and J. G. Kuhry. 1991. *Biol. Cell.* 73:131–138). As such, TMA-DPH displays particular properties mainly due to partition between membranes and aqueous media. From these properties, original arguments can be inferred in favor of the maturation model for the endocytic pathway, against that of pre-existing compartments, in L929 cultured mouse fibroblasts. (*a*) TMA-DPH labeling is seen to progress from the cell periphery to perinuclear regions during endocytosis without any noticeable loss in fluorescence intensity; with a vesicle shuttle model this evolution would be accompanied by probe dilution with a decrease in the overall intracellular fluorescence intensity, and the labeling of the inner (late) compartments could in no way become more intense than that of the peripheral (early) ones. (*b*) From TMA-DPH fluorescence anisotropy assays, it is concluded that membrane fluidity is the same in the successive endocytic compartments as in the plasma membrane, which probably denotes a similar phospholipidic membrane composition, as might be expected in the maturation model. (*c*) TMA-DPH internalization and release kinetics are more easily described with the maturation model.

ENDOCYTOSIS is a constitutive mechanism whereby most eukaryotic cells, to a variable extent, internalize external fluid (fluid phase endocytosis) and certain membrane receptors whether bound to their ligand or not (receptor mediated endocytosis) via plasma membrane carrier vesicles (for review see van Deurs et al., 1989; Steer and Hanover, 1991). Endocytic vesicles generally originate from particular regions of the plasma membrane called *coated pits* which on the cytoplasmic side are covered by a clathrin coat. Once formed, endocytic vesicle rapidly lose this coat and their content is sequentially delivered to elements of the endosomal compartment namely, a series of vacuoles with decreasing luminal pH, including early (sorting) endosomes, late endosomes, and, finally, lysosomes containing acidic degrading enzymes. Endocytosis has been extensively investigated over the past 15 years (three to four hundred papers a year alone on the key word endocytosis since 1984; source Medline). Because of the broad range of the subject, studies have followed various specific directions, among them, morphological, morphometric, and kinetic aspects (for reviews see Besterman et al., 1981; Steinman et al., 1983; Helenius et al., 1983; Thilo, 1985; Marsh et al., 1986; Griffiths et al., 1989); biochemical and functional properties of endocytic vesicles and of the clathrin coat; the role of the latter as a receptor filter; the vesicle uncoating process (for reviews see Goldstein et al., 1985; Brodsky, 1988; Heuser, 1989; Keen, 1990; Pearse and Robinson, 1990; Brodsky et al., 1991; Smythe and Warren, 1991; Schmid, 1993; Anderson, 1993; Wang et al., 1993); compartment acidification mechanisms (for reviews see Mellman et al., 1986; Anderson and Orci, 1988; Murphy, 1988; Yamashiro and Maxfield, 1988; Feng and Forgac, 1992); modalities of fusion events (for reviews see Mayorga et al., 1989; Wessling-Resnick et al., 1990; Wilson et al., 1991); the sorting of lysosomal enzymes and the role of mannose-6-phosphate receptors (for reviews see Geuze et al., 1988; Kornfeld and Mellman, 1989; Griffiths et al., 1990; Von Figura, 1991; Méresse and Hoflack, 1993); the influence of temperature (for reviews see Haylett and Thilo, 1991; Illinger et al., 1991) and of cytoskeleton integrity (for reviews see Sandvig and van Deurs, 1990; Bomsel et al., 1990; Illinger et al., 1991); and the importance of the cell cycle (Tuomikoski et al., 1989).

Address all correspondence to Dr. Jean-Georges Kuhry, Laboratoire de Biophysique, URA 491 du CNRS, Faculte de Pharmacie, 74 route du Rhin, B.P. 24, 67401 Illkirch Cedex, France.

© The Rockefeller University Press, 0021-9525/94/05/783/12 $2.00

This paper focuses on the mechanisms whereby the endocytosed material is transferred to the successive endosomal compartments and to lysosomes. This question is fundamental for an understanding of cell membrane economy. It was first raised by Helenius et al. (1983), who proposed two models. In the so-called vesicle shuttle model, endocytic compartments pre-exist as specific stable entities and sequential transfer of their contents occurs via specialized carrier vesicles. The alternative maturation model postulates that endocytic vesicles, after shedding their clathrin coat, fuse to form early endosomes; the latter mature gradually into late endosomes and lysosomes, thanks to competing vesicle inflow via the secretory pathway (*trans*-Golgi network) and the outflow of recycling vesicles. The evolution is often thought to be determined by the spatial organization of the pathway. Both models have received appropriate experimental support (for reviews see Hubbard, 1989; Griffiths and Gruenberg, 1991; Murphy, 1991).

Arguments in favor of the pre-existence of the compartments are based on the observation of selective fusions in cell-free assays and of specific associations of biochemical markers with each type of compartment. It has been shown that, while early endosomes can fuse with each other, this does not occur with late endosomes; carrier vesicles from early endosomes can not fuse between themselves, nor fuse back with early endosomes, but can fuse with late endosomes (Gruenberg and Howell, 1989; Gruenberg et al., 1989; Bomsel et al., 1990; Gorvel et al., 1991). On the other hand, the cytosolic GTP-binding proteins *rab 5* and *rab 7*, which are assumed to play a regulatory role in the endocytic pathway, have been shown to associate specifically with early and late endosomes, respectively; neither of these proteins has been detected in carrier vesicles (Schmid et al., 1988; Beaumelle et al., 1990; Gorvel et al., 1991).

Typical arguments for the maturation model are based on experiments with sequentially internalized endocytosis markers (Roederer et al., 1987; Salzman and Maxfield, 1988; Ward et al., 1990; Stoorvogel et al., 1991; Dunn and Maxfield, 1992): while pulse-internalized probes were initially accessible to fusion, fusion accessibility rapidly decreased with time. Particularly conclusive are the results of Dunn and Maxfield (1992), with DiI- and -DiO-LDL (LDL conjugated with 3,3′-dioctadecyl-indocarbocyanine and 3,3′-dioctadecyl-oxacarbocyanine, respectively). They used digital image analysis, allowing individual endosomes to be distinguished. The colocalization of DiI- and -DiO-LDL decayed exponentially with a chase-half-time of 6 min between the two pulses. Another kind of argument was put forward by Roederer et al. (1990), who showed that isolated endosomes in vitro could autonomously increase their buoyant density up to that of lysosomes. One difficulty with the maturation model was the apparently specific targeting of endosomal luminal contents on lysosomes, while membrane-associated molecules (e.g., receptors) preferentially recycled towards the cell surface. In this respect, it has been shown recently (Mayor et al., 1993), with quantitative fluorescence microscopy of both membrane bulk markers and labeled receptors, that this specificity did not require molecular recognition signals. It simply resulted from the geometric features of early (sorting) endosomes. These display a tubulo-vesicular structure, with most of the membrane surface concentrated in narrow tubular extensions, which naturally tend to bud off; soluble contents (ligands) mostly remain in the volumic vesicular part, where they mature until the final lysosomal step.

Our contribution to this question stems from the particular properties of the fluorescence probe 1-(4-trimethylammonium)-6-phenyl-1,3,5-hexatriene (TMA-DPH)[1] when it is used as an endocytic pathway marker. TMA-DPH was introduced for fundamental purposes by Prendergast et al. (1981) as a model molecular rotor in phospholipidic membranes. Subsequently, we showed that TMA-DPH interacted with living cells by instantaneous partition between the plasma membrane (probe fluorescent) and the external medium (not fluorescent) (Kuhry et al., 1983, 1985). TMA-DPH therefore became widely used as a probe for plasma membrane fluidity determinations by measuring fluorescence anisotropy on living cells (see references in Haugland, 1992). Being associated with the plasma membrane, it was expected to follow this membrane in its intracellular endo- and exocytic traffic and to behave as an endocytic bulk membrane marker. This was in fact established (Illinger et al., 1990*a*, 1991), and it appeared that TMA-DPH, as such, displayed original properties based mainly on the water/membrane partition. These properties will be reviewed here. The water/membrane partition equilibrium implies, for instance, that TMA-DPH fluorescence intensity is determined by its concentration in solution and by the surface of the membrane in contact with this solution. This allows the correlation of changes in the surface/volume ratio, during the endocytic pathway with possible changes in fluorescence intensity, and, on that basis, a prediction of the evolution of TMA-DPH intracellular labeling according to each of the two models. On the other hand, thanks to the same partition property, membrane fluidity can be assessed separately from TMA-DPH fluorescence anisotropy measurements, both in the peripheral and in the internalized membrane. The evolution of this parameter is also expected to differ in the two models. Data obtained on *L929* mouse fibroblasts with this tool showed that the bulk intracellular membrane traffic in endocytosis could scarcely be described with a vesicle-shuttle model, but was much easier to interpret in terms of "maturation."

Materials and Methods

Cell Cultures

L929 mouse fibroblasts, a cell line currently used in our laboratory, were cultured as adherent monolayers in 25-cm^2 plastic dishes (Costar Corp., Cambridge, MA) in DME (4.5 g/l D-Glucose, 3.7 g/l $NaHCO_3$) with 10% heat decomplemented FCS (Biolab, Euromedox, France), 1% 100 mM sodium pyruvate, 1% 200 mM L-Glutamine and antibiotics (penicillin 50 U/ml-streptomycin, 50 μg/ml, a preparation henceforth referred to as DM10F (according to Swanson et al., 1987). The cultures were kept in a water-saturated atmosphere of 8% CO_2 in air, at 37°. These particular conditions were required for the production of the L929 supernatant enriched in Macrophage Colony Stimulating Factor used in other studies (Illinger et al., 1990*b*). For the assays, the cells were recovered by trypsination with 0.25% trypsin in PBS without Ca^{2+}, Mg^{2+} (henceforth referred to as PBS), and their viability (>95%) was determined by Trypan blue exclusion.

1. *Abbreviations used in this paper*: C_6-NBD-SM, N-[N-(7-nitro-2,1,3-benzoxadiazol-4-yl]-ε-aminohexanoyl)-sphingosylphosphorycholine; TMA-DPH, 1-(4-trimethylammonium)-6-phenyl-1,3,5-hexatriene.

TMA-DPH Cell Labeling and Fluorescence Microscopy

L929 cells (typically 10^5/ml) in 2 ml DM10F were allowed to adhere on microscope slide flasks (Nunc). For the observation of plasma membrane labeling, cells were incubated for a short time (10 s) at room temperature with TMA-DPH (Molecular Probes Inc., Eugene, OR) 2×10^{-6} M in PBS or in DM10F from a 4×10^{-3} M stock solution in dimethylformamide. The unwashed slide was then transferred to the microscope and observed.

For the labeling of internalized membrane, the cells were incubated in slide flasks at 37°, with TMA-DPH 2×10^{-6} M in DM10F for the desired time, and then washed by gently shaking the slide in PBS for a few seconds. This allowed the elimination of peripheral labeling, thanks to partition equilibrium, whereas the intracellular probe fraction, enclosed in endocytic compartments, was protected from the washing effect.

The observations were performed with an Optiphot 2 (Nikon) photomicroscope, equipped for epifluorescence, using 335–345 nm excitation, with the barrier filter at 400 nm. Considerable TMA-DPH photobleaching was induced by the UV excitation light (Duportail and Weinreb, 1983), so it was not possible to both focus on and photograph the same field. The procedure adopted was to focus on one field, and then to photograph the immediately adjacent field. Photographs were taken on Kodak T-Max P3200 films used at a sensitivity of 1600 ASA.

A double-labeling technique with acridine orange was used to stain the highly acidic cell compartments (late endosomes, lysosomes, and, incidentally, nucleoli) (Rolland et al., 1976). A 5 μg/ml acridine orange (Sigma Chem. Co., St. Louis, MO) solution in PBS was carefully added to the slide under the microscope after observation of TMA-DPH labeling. The typical orange fluorescence was then observed on the same field after a 4-min incubation. The filters used were 510–560 nm for excitation, and over 590 nm for emission. Under these conditions, no interference between the two labelings could occur.

TMA-DPH Cell Internalization and Release Kinetics

These kinetics were monitored by fluorescence intensity measurements.

Internalization. 5×10^5 cells were allowed to adhere in 3.5-cm diam Petri dishes in the presence of 2 ml DM10F and thereafter incubated at 37° for various times with 2×10^{-6} M TMA-DPH in the same medium. At the end of incubation, the cell layers were washed four times for 5 s with cold PBS to remove peripheral labeling. The TMA-DPH fluorescence intensity was measured immediately after recovery of the cells in 2 ml PBS by gentle scraping with a cell lifter (Costar Corp.) which left them undamaged. Cell viability was regularly controlled at this step, and after the measurements, it was found to be unaltered. Here, it should be mentioned that other tools, such as "cell scrapers" (same origin) were not harmless and caused partial disruption. Homogeneous suspensions were required for the relevant measurements, which were performed at room temperature, under moderate stirring, with an MPF-66 Perkin-Elmer spectrofluorimeter (excitation 360 nm, emission 435 nm, bandwidth 5 nm). In this way, the TMA-DPH intracellular fluorescence intensity could be obtained less than 1 min after the end of incubation. For the sake of standardization, data have been expressed as % of the fluorescence intensity of the peripheral labeling, measured in parallel on unwashed cells at the same density, after a 10-s incubation at room temperature, with TMA-DPH, at the same concentration, in PBS. The reason why PBS was used for the measurements instead of DM10F, was that the medium and the serum induced disturbing screening effects. These screening effects result from the reduction of the excitation light intensity by absorbance and scattering by the components of DM10F. Their occurrence was demonstrated by the use of low optical path quartz cuvettes (0.2 instead of 1.0 cm). Fluorescence spectra, however, remained qualitatively unchanged, denoting the absence of quenching effects. The background light intensity, measured systematically on unlabeled controls, was negligible. It is noteworthy that L929 cells displayed no detectable autofluorescence under UV excitation light.

Release. After the desired incubation time for TMA-DPH uptake (as above), the cell layers were washed with PBS to remove the peripheral labeling and reincubated for various times in TMA-DPH-free DM10F, and the fluorescence intensity was measured as above.

Membrane Fluidity Assays

Membrane fluidity was assessed from TMA-DPH fluorescence anisotropy measurements. The same cell preparation was used to measure the membrane fluidity of the plasma membrane, on unwashed cells, and that of the endocytosed membrane, on washed cells. With fluorescence anisotropy, membrane fluidity is interpreted in terms of hindrance to rotational motion of the probe, since it is embedded in the constraining phospholipidic membrane array (Kinosita et al., 1977; van Blitterswijk et al., 1981). Fluorescence anisotropy is the parameter $r = I_{//} - I_X / I_{//} + 2I_\perp$, where $I_{//}$ and $I_\perp$ represent the components of the light intensity emitted, respectively, parallel and perpendicular to the direction of the vertically polarized excitation light. Basically, r values range from 0.0 to 0.4, the higher values corresponding to a high lipidic order and vice-versa.

The measurements were performed on two kinds of samples: cells incubated for 10 s with TMA-DPH (2×10^{-6} M) in PBS and recovered without washing, to evaluate the membrane fluidity in the plasma membrane; cells incubated with TMA-DPH in DM10F at 37° for 1 min and washed (TMA-DPH pulse). This short TMA-DPH uptake time was still long enough to ensure significant internalization (very early endocytosis). The fluorescence anisotropy was then measured after various reincubation times, at 37° in TMA-DPH-free medium, to monitor the evolution of membrane fluidity during the progression of the endocytic process. Measurements were made at room temperature, under gentle stirring, with an SLM 8000 spectropolarofluorimeter, after recovery of the cells in PBS. Each sample was measured 10 times for 2 s. Homogeneous cell suspensions were required for relevant statistics and precision. Trypan blue exclusion tests performed after the measurements, on the cell suspensions from the quartz cuvettes, indicated viability levels higher than 95%.

The background light (scattered unresolved excitation light) was negligible (i.e., <1%) for the peripheral labeling. It was not so for the fluorescence of the probe internalized, when it could be as high as 15%. This contribution was taken into account in applying the additive property of the anisotropy parameter, as described earlier (Kuhry et al., 1985), and required careful measurement of unlabeled controls. An additional experiment confirmed that raising the TMA-DPH concentration to 6×10^{-6} M (lower noise contribution) gave exactly the same results after correction.

The approach used was steady-state anisotropy, i.e., under continuous illumination, which is the most common and the easiest. However, in this case, the results are known to depend on the fluorescence lifetime (van Blitterswijk et al., 1981). Thus, adequate interpretations need complementary lifetime determinations. These were performed with a monofrequency phase and modulation technique (Wu and Lentz, 1991) using an SLM 48000 TM instrument. The modulation frequency was set at 30 MHz and diphenylhexatriene in tetrahydrofuran was used as a reference (τ = 6.7 ns, Poujet et al., 1989). This method proved sufficiently accurate for the purpose and was consistent with the rapid evolution of the system studied.

Results

This section brings together all the experimental data obtained with TMA-DPH, which allow a distinction to be drawn between the maturation model for endocytosis and the pre-existing compartments one. These include (*a*) the properties which proclaim TMA-DPH as an endocytic marker, (*b*) the particular features of TMA-DPH as such a marker, (*c*) the intracellular labeling evolution with this probe, (*d*) TMA-DPH internalization and release kinetics, and (*e*) fluorescence anisotropy results. Not all experimental observations are original. Some of them (internalization and release kinetics) have been partly described in earlier papers (Illinger et al., 1990*a*, 1991). However, even in this case, the experiments have been deliberately repeated here in order to build up a coherent overall scheme for the present purpose.

TMA-DPH Is an Endocytic Marker

It is internalized in living cells only by endocytosis: (*a*) in contact with cells, TMA-DPH is instantaneously incorporated into the plasma membrane. This is shown in Fig. 1 *a* for L929 cells, observed after 10 s incubation with TMA-DPH 2×10^{-6} M in PBS. This property is due to the positive charge of the molecule. Using fluorescence inhibitors, Cranney et al. (1983) showed that the incorporation is limited to the external leaflet of the membrane. Actually,

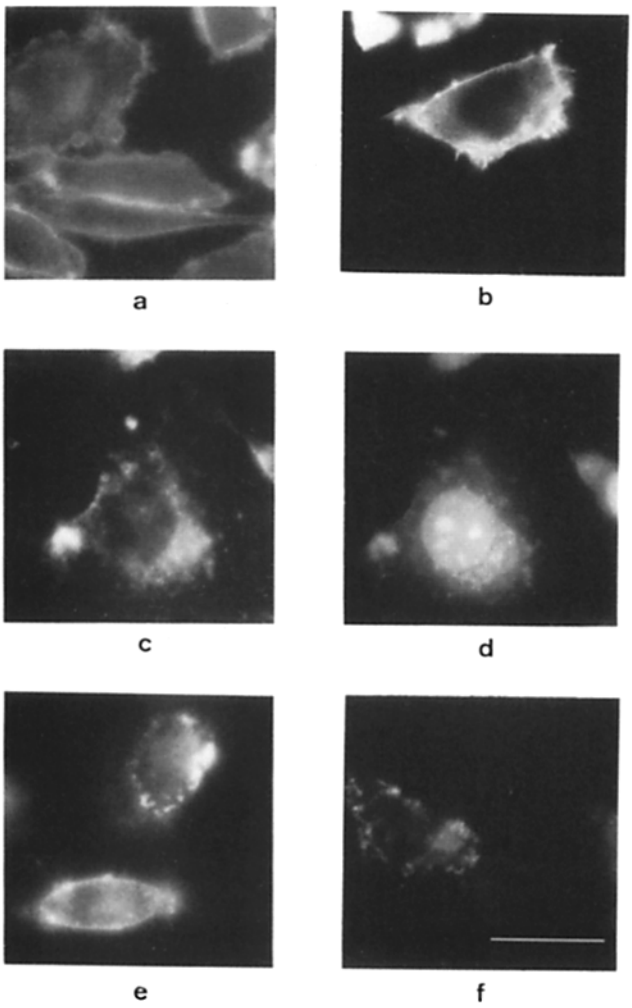

Figure 1. TMA-DPH labeling features in L929 cells. 2×10^5 L929 cells on microscope slide flasks were (*a*) incubated for 10 s with TMA-DPH (2×10^{-6} M) in PBS, and observed immediately for peripheral fluorescence labeling. (*b*) Incubated with TMA-DPH (same concentration) in DM10F at 37° for 20 min, and observed without washing. Comparison with the peripheral labeling shows that nuclear membrane is not labeled. (*c*) Incubated with TMA-DPH (same concentration) for 90 min, at 37° and washed for observation of intracellular labeling. (*d*) Double labeled with acridine orange 5 μg/ml, added under the microscope after TMA-DPH observation (same field). (*e–f*) Pulse-chase experiment (*e*) cells incubated for 3 min with TMA-DPH (5×10^{-6} M) at 37° and washed. (*f*) Same sample reincubated in TMA-DPH-free medium at 37° for 30 min (not the same field). Bar, 10 μm.

TMA-DPH undergoes partition between the membranes and the eternal medium. When the cell preparations are washed after contact with TMA-DPH, the probe is extracted from the membrane with a loss of fluorescence; under the microscope, the fields observed are then totally black (not represented). The consequence of these properties is that TMA-DPH, being associated to the plasma membrane, is bound to follow this membrane in the intracellular traffic.

(*b*) Fig. 1 *c* shows the labeling features of L929 cells incubated for 90 min with TMA-DPH (2×10^{-6} M) in DM10F at 37°, and then washed with PBS to extract the peripheral plasma membrane labeling. The intracellular labeling appears granular and more localized in the perinuclear region. Double labeling with acridine orange, as described in Materials and Methods, shows important colocalization (Fig. 1 *d*) of the two markers, indicating that TMA-DPH is concentrated in lysosomes and highly acidic late endosomes.

(*c*) The evolution of intracellular labeling after a TMA-DPH pulse-chase is seen in Fig. 1, *e* and *f*. L929 cells were incubated for 3 min with TMA-DPH (5×10^{-6} M) in DM10F at 37° (the higher probe concentration was needed for sufficient observation sensitivity). The preparation was then washed, so as to remove the plasma membrane labeling. Immediately after the chase, the labeling is typically peripheral, submembranar (Fig. 1 *e*). When the same preparation is further reincubated in TMA-DPH-free DM10F at 37° for 30 min (Fig. 1 *f*), the labeling appears to have moved toward inner parts of the cells. This result (see Discussion) is actually one of our arguments for preferring the maturation model for endocytosis.

(*d*) TMA-DPH internalization kinetics in L929 cells are greatly reduced during mitosis (Illinger et al., 1994), as reported by other authors, for endocytosis (Berlin and Oliver, 1980).

Altogether, these features strongly suggest that TMA-DPH is internalized into the cells via endocytosis.

(*e*) It was then important to examine whether or not endocytosis was the only mechanism for TMA-DPH internalization. If other mechanisms, such as passive diffusion or transbilayer movement (Flip-Flop), were to contribute significantly to this internalization, TMA-DPH would be present in the cytosol and would label the external leaflet of all intracellular membranes, among them, that of the nuclear membrane. Fig. 1 *b* clearly shows that the nuclear membrane is not labeled. Here the cells were incubated for 20 min with TMA-DPH (2×10^{-6} M) in DM10F at 37° and deliberately not washed. The nucleus appears in contrast with the surrounding labeling, but comparison with the plasma membrane reveals the absence of nuclear membrane labeling. The absence of TMA-DPH from cytosol was confirmed by the following experiment. When cells were submitted to controlled disruption (preserving organelle integrity) after extensive TMA-DPH uptake and washing, the fluorescence intensity was found to be exactly the same as in intact cells. This means, on the grounds of the water/membrane partition property, that intracellular TMA-DPH is protected from interaction with the cytosol, which suggests it is present only in closed structures (endocytic compartments).

(*f*) TMA-DPH internalization and release kinetics (see Fig. 3), in particular the early inflexion of the curves, may not be explained by either Flip-Flop or diffusion. But, as discussed below, they are consistent with the kinetics of intracellular membrane traffic.

It thus emerges that TMA-DPH can be used as an endocytic marker. As such, it displays original properties discussed hereafter. It should be mentioned that other laboratories now use TMA-DPH for monitoring endocytosis in other cell types (Padh et al., 1993; Courtoy, 1991; International Institute of Cellular and Molecular Pathology, Bruxelles, Belgium, personal communication).

TMA-DPH Properties As an Endocytic Marker

(*a*) It is a bulk membrane marker. Instantaneously incorporated into membranes, it shares hydrophobic interactions (through its apolar moiety) with the membrane phospholipidic acyl chains, and is fluorescent only in membranes. However, it is not a phospholipid analogue and does not interfere with phospholipid metabolism.

(*b*) Unlike phospholipid fluorescent analogues (for review see Kok et al., 1990; Koval and Pagano, 1989), the presence of TMA-DPH in membranes implies equilibrium with its aqueous non-fluorescent solution form (see appendix). Since the fraction incorporated in membranes is low (appendix) it should be considered that whatever the circumstances, the solution plays the role of a TMA-DPH reservoir and that the membrane in contact with the solution, i.e., the support for the fluorophore is constantly dependent on this reservoir. This point is important for the further developments in this paper and will be discussed in detail below.

(*c*) TMA-DPH is an atypical marker for endocytosis, i.e., devoid of any type of interaction with specific receptors. Its presence at the concentration used does not affect the kinetics of the phenomena studied. As a matter of fact, TMA-DPH internalization rates remained proportional to the probe concentration in the range examined (5×10^{-7} M to 2×10^{-5} M) (not represented).

(*d*) It is not metabolized, and the fluorescence intensity is insensitive to pH changes, at least from pH 3 to 9. It displays no cytotoxicity at all. The proliferation rate and viability levels of L929 cells were not modified when 5×10^{-6} M TMA-DPH were present for more than 60 h. This was not true for the parent molecule, DPH, which began to induce cell mortality after 2 h. The reason could be that TMA-DPH, contrary to DPH, is trapped in endocytic compartments.

(*e*) TMA-DPH is very rapid to use: significant internalization can be measured in L929 cells as early as 30 s after the addition of the probe. It requires much lower concentrations than some fluid phase markers: typically 1 μg/ml instead of ~1 mg/ml for Lucifer Yellow (Swanson, 1987).

Elementary Models for TMA-DPH Labeling of the Endocytic Compartments

TMA-DPH partition equilibrium is written $[\text{TMA-DPH}]_{mb}/[\text{TMA-DPH}]_{aq} = K$, where $[\text{TMA-DPH}]_{mb}$ and $[\text{TMA-DPH}]_{aq}$ stand, respectively, for the membranar and aqueous concentration of the probe. In terms of fluorescence intensity (I_f) this is equivalent (see appendix) to $I_f = kcs$ (c, probe concentration; s, membrane surface in contact with the probe).

The first event in endocytosis is the formation of the endocytic vesicle. In this case, c represents the initial TMA-DPH concentration and s the vesicle membrane area (inner leaflet) (Fig. 2 *a*). How the fluorescence evolves as the endocytic pathway progresses will depend on further probe dilution or membrane surface changes. So, the evolution of the fluorescence intensity could be an interesting support for discussing mechanisms. However, the basis for such discussion could, a priori, be subject to two criticisms: the value of the partition constant K may change from one type of membrane to another; the kinetics of the partition equilibrium establishment may depend on geometric factors; they could be slower, for instance, in narrow tortuous tubules than in large spherical compartments. Fortunately, these reserves can be laid aside. We have shown in the laboratory (Duportail, G., unpublished data) that the incorporation of TMA-DPH is seven times higher in small unilamellar phosphatidylserine (negatively charged) vesicles than in phosphatidylcholine (no net charge) ones, but this is an extreme case. In biological membranes, we have for instance assessed K at 1.0 ×

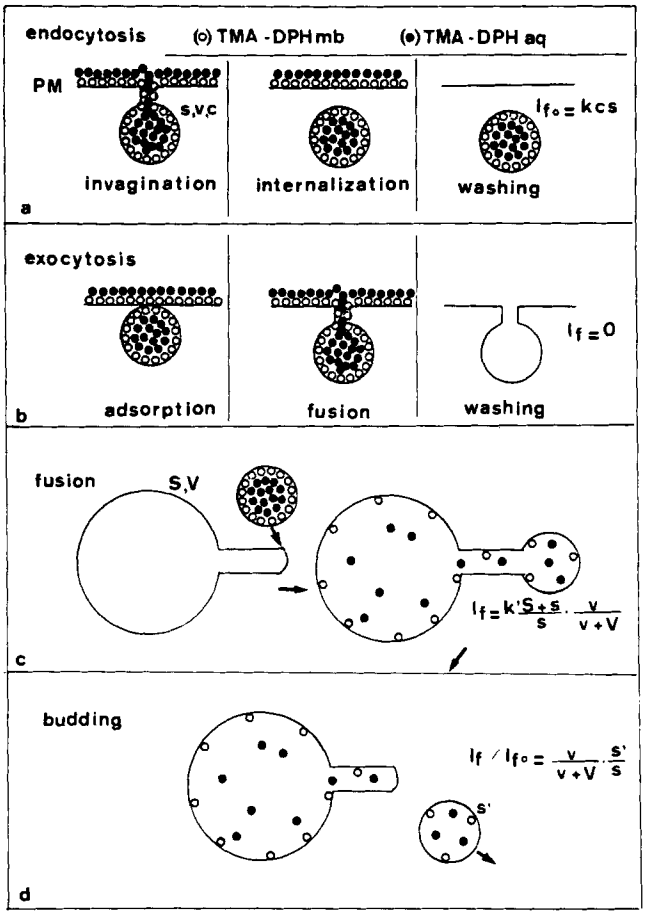

Figure 2. Elementary models for the interpretation of TMA-DPH labeling features. When TMA-DPH is added to the cell preparation it is instantaneously partitioned between the external aqueous medium (probe not fluorescent) and the external leaflet of the plasma membrane (probe fluorescent). No significant passive diffusion or transbilayer movement occurs across this membrane. (*endocytosis*) The membrane invaginates and engulfs external TMA-DPH in a vesicle which is internalized. In this vesicle, TMA-DPH is partitioned between the internal leaflet of the membrane vesicle and the medium engulfed. Because of this partition equilibrium, the fluorescence intensity internalized by the vesicle is proportional (see Appendix) to the vesicle surface and to TMA-DPH total concentration, which is approximately equal to that in the external medium. (*exocytosis*) Since the measurements are performed after washing, exocytosis results in loss of the fluorescence intensity of the vesicles concerned. (*fusions*) Because of the partition equilibrium, the fluorescence intensity after fusion depends on the surface/volume ratio of the partners in fusion. (*budding events*) For the same reason, the fluorescence intensity of a budding vesicle is generally much lower than that of an incoming endocytic vesicle.

10^5 in L929 cells and 1.2×10^5 in mouse bone-marrow-derived macrophages, hardly a significant difference, while TMA-DPH incorporation was found to be identical in direct and inside-out erythrocyte ghosts (unpublished data). On the other hand, geometric factors do not seem to have much influence on the kinetics of the partition equilibrium. For example, to determine the membrane-incorporated fraction of TMA-DPH in L929 cells, we measured the concentration of the probe in a cell supernatant by UV absorption and the result was the same for a cell suspension after low-speed centrifugation as for a confluent cell layer after 10 s of contact (distance from the cells to the plastic support 0.006 μm) (Grinnell, 1978). Other studies in our laboratory have indicated that changes in cell shape induced in platelets by ADP, from the discoïd to the highly contorted shape (Kubina et al., 1987) and in macrophages by interferon-gamma (unpublished data), did not modify TMA-DPH incorporation features. Another question regarding geometric factors is the possible a priori influence of the relative volume of the TMA-DPH reservoir. More precisely, is it safe to assume that the TMA-DPH distribution coefficient is comparable in plasma membranes in contact with a large volume of extracellular medium, and in endocytic vesicles, with a considerably smaller volume. This question could be resolved thanks to a simple experiment performed in our laboratory. Small unilamellar phosphatidylcholine vesicles were prepared under exactly the same conditions, either with TMA-DPH in the buffer or without it. In the latter case, TMA-DPH, at the same concentration was added after the preparation. Within the limits of experimental error, the fluorescence intensity in the first preparation (in and out labeling) was found to be twice that in the second (outer labeling only).

Thus, it may be assumed that when transfer occurs between endocytic compartments, TMA-DPH instantaneously occupies the whole available luminal volume and from there immediately equilibrates with the whole available membrane, with little change in the partition coefficient.

Fig. 2 shows schematically how, on that basis, fluorescence intensity may be influenced in some simple cases: (*a*) exocytosis of TMA-DPH-labeled vesicles (2 *b*) results in the loss of the corresponding fluorescence, since cells are washed before measurement. (*b*) Fusion events (2 *c*) result in TMA-DPH dilution but this effect is partially counterbalanced by the increase in membrane surface. The actual change in fluorescence depends on the surface/volume ratio before and after fusion. This ratio may not be changed, e.g., in fusion between vesicles of the same size, or in fusion between vesicles and larger elements which have themselves been formed by multiple vesicle fusions (endosomes in the maturation model). The fluorescence intensity is then unchanged. On the contrary, fusions with elements with a low surface/volume ratio (e.g., spherical-shaped compartments) result in a decrease in fluorescence intensity. For instance, the fusion of a labeled vesicle (radius r) with a large spherical compartment (radius R) decreases fluorescence by r/R. The fluorescence intensity may even increase: this might occur, for instance, when an unlabeled membrane comes into contact with the probe, with little change in volume (not represented). This possibility will be considered for instance in the discussion of the maturation model to explain the constant part of the TMA-DPH release curves (see below). This was also the basis of the method developed in our laboratory for monitoring stimulated exocytosis by a simple increase in fluorescence intensity (Bronner et al., 1986). (*c*) Budding events (2 *d*) themselves do not change the overall intracellular fluorescence intensity. Comparison of a labeled endocytic vesicle fusing with a compartment, and an element budding from that compartment, indicates that the fluorescence intensity of the budding element is always lower than that of the incoming vesicle.

TMA-DPH Internalization and Release Kinetics

The curves in Fig. 3 represent (*closed symbols*) the evolution of intracellular fluorescence intensity, measured after cell washing, as a function of the incubation time with TMA-DPH at 37° (internalization kinetics), and, (*open symbols*) the evolution of fluorescence intensity after probe uptake (10 and 30 min), in TMA-DPH-free DM10F, also at 37° (release kinetics). For the sake of standardization, the results have been related to the fluorescence intensity of the peripheral labeling measured in parallel, on unwashed cells. Both curves are biphasic.

(a) Internalization. The intracellular fluorescence intensity is the result of all events of the endocytic pathway, which occurred during the incubation with TMA-DPH. For short incubations (<5 min), these are mainly limited to the formation of endocytic vesicles, accounting for the rapid initial increase in fluorescence intensity: most recycling vesicles are then unlabeled. With increasing incubation time, the flow of recycling labeled vesicles increases and this slows down the increase in fluorescence intensity (inflexion of the curve) until an equilibrium. The second part of the curve (lower slope), observed for longer incubations, has been shown previously (Illinger et al., 1991) to be markedly

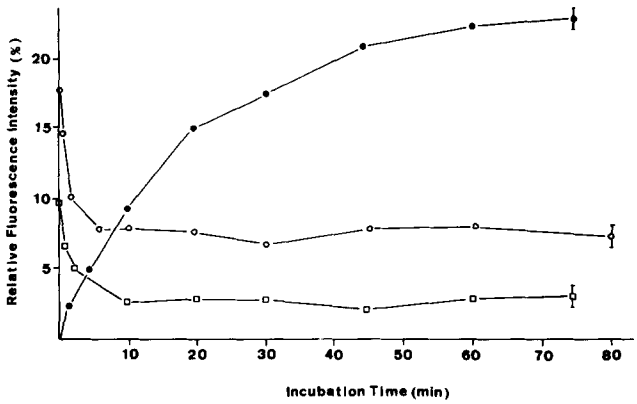

Figure 3. TMA-DPH internalization (*closed symbols*) and release (*open symbols*) kinetics in L929 cells. (*a*) 5×10^5 adhered L929 cells were incubated, at 37°, for various times with TMA-DPH (2×10^{-6} M), and then washed to remove the peripheral labeling. After the recovery of cells as a suspension in PBS, the fluorescence intensity was measured at 435 nm (excitation 360 nm) and the results were expressed as % of the fluorescence intensity of the peripheral labeling, measured in parallel on unwashed cells after 10 s incubation in PBS. (*b*) A first incubation for the desired time with TMA-DPH was done as above, and the cells were then reincubated, at 37°, after washing, in fresh medium. The relative fluorescence intensity is represented as a function of time after the end of the first incubation. Error bars denote average SD from four determinations.

influenced by temperature, and to be totally suppressed below 15°. This suggests that the mechanisms involved are dependent on fusion events, which are known to be particularly sensitive to decreases in temperature and which no longer occur below some critical temperature in this range (Dunn et al., 1980, 1986; Hare, 1988; Haylett and Thilo, 1991). The slope in the second part of the curve becomes constant after ~30 min and remains the same for actually much longer than represented in the figure (assays performed up to 10 h). Nothing really spectacular in these trends of curves obviously argues against any of the two models.

(b) Release. The curves display first a rapidly decreasing portion (3–5) min after TMA-DPH chasing, and then a surprisingly constant portion, which, here again, lasts for much longer than represented in the figure (assays performed the day after). The level of this lower constant limit increased with the incubation time with TMA-DPH. Assays performed for shorter incubation times (2 and 5 min) gave similar curves (not represented). The first, decreasing portion of the curves probably denotes a too early (observed even for 2 min incubations) and too rapid effect, to be attributed to recycling from endosomal compartments, despite the rapid kinetics of these mechanisms (Mayor et al., 1993). Rather, this effect could be attributed to direct recycling of newly internalized endocytic vesicles, a mechanism referred to as "reversible pinocytosis" by other authors (Besterman et al., 1981; Daukas et al., 1983; Storrie et al., 1984; Goud et al., 1984). This is of minor importance in the present concern. The constant portion of the curve raises more constructive questions. Obviously, no more TMA-DPH is internalized (probe-free external medium), but important recycling certainly occurs from the endosomal compartment, and this happens without noticeable decrease in intracellular fluorescence intensity. This, at least, assumes the decrease in fluorescence intensity to be balanced by the replacement of the endosomal membrane consumed in recycling, with negligible probe dilution. This point will be discussed in detail (see Discussion) and it will be shown that this requirement may be satisfied with a maturation model, but not with that of preexisting compartments.

Fluorescence Anisotropy Data

Fluorescence anisotropy measurements were done to assess membrane fluidity. As a matter of fact, the evolution of membrane fluidity differs predictably in the two models. With pre-existing compartments it should vary when the probe is transferred from one compartment to another. Conversely, with the maturation model it would be expected to remain the same as in the plasma membrane, throughout the endocytic pathway (see Discussion).

Fig. 4 represents the evolution of the fluorescence anisotropy after a 1-min TMA-DPH pulse, followed by rapid cell washing and further incubation in TMA-DPH-free DM10F, i.e., the evolution of the fluorescence anisotropy during the endocytic pathway, from the very beginning of the process. Immediately after cell washing (<30 s), r was strikingly high 0.336 ± 0.003, and then rapidly (half-time, 1 min) decreased to a lower stable value of 0.286 ± 0.03; this value remained constant for hours and was identical, within the limits of experimental precision, to the value of TMA-DPH fluorescence anisotropy in the plasma membrane, measured on unwashed cells after a 10-s incubation with TMA-DPH in PBS. These results seemed so remarkable that we repeated the experiment with another cell type in use in the laboratory, namely mouse-bone-marrow-derived macrophages, prepared as described earlier (Illinger et al., 1990*b*). Similar curve trends were observed, with an initial value of 0.312 ± 0.03 and a lower limit of 0.275 ± 0.003, the latter also being the same as the overall value in the plasma membrane.

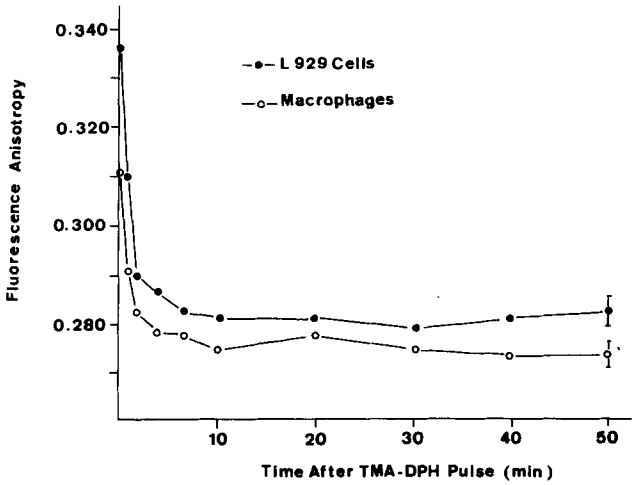

Figure 4. Evolution of TMA-DPH fluorescence anisotropy as a function of time after a 1-min uptake of the probe by L929 cells and macrophages. Adhered cells (5×10^5) were incubated for 1 min with TMA-DPH (2×10^{-6} M) at 37° and extensively washed to remove peripheral labeling. They were then reincubated for various times, at 37°, in TMA-DPH-free medium and recovered, by gentle scraping, in 2 ml PBS, for the fluorescence anisotropy measurements. The results are represented as a function of time after the TMA-DPH pulse. Error bar denotes average SD from four determinations. For comparison, TMA-DPH fluorescence anisotropy in the cell plasma membrane was measured on unwashed cells incubated for 10 s with TMA-DPH (2×10^{-6} M) in PBS, and recovered by gentle scraping.

No changes in fluorescence lifetimes were observed in these experiments. They displayed constant values of 5.6 ± 0.3 ns in L929 cells and 6.2 ± 0.3 ns in macrophages, independently of the time after cell washing. These values were also the same for TMA-DPH in the plasma membrane (unwashed cells). Thus, the results could be validly interpreted in terms of membrane fluidity. They show that the fluidity of the membrane internalized is the same as that of the bulk plasma membrane, all along the endocytic pathway, except for the very early phase. Several arguments led us to assume that the higher fluorescence anisotropy in these early instants, was actually due to increased lipidic order in the endocytic vesicle membrane induced by interactions with the clathrin-coat; (*a*) the clathrin-uncoating process and the decrease in fluorescence anisotropy display similar kinetics (Pearse and Bretscher, 1981; Helenius et al., 1983; Paddenberg et al., 1990; Smythe and Warren, 1991); (*b*) when the clathrin coat is released, the expected membrane fluidity level in the uncoated vesicle should be the same as in the overall plasma membrane, where vesicles originate from. This is in fact observed; (*c*) membrane fluidity studies have been performed in another laboratory (Liaubet, A., and M. Charlier, Centre de Biophysique Moléculaire, Orléans,

France, manuscript submitted for publication) on purified coated (cv) and uncoated (uv) bovine brain endocytic vesicles, using diphenylhexatriene and pyrene derivatives as markers. Membrane fluidity was found to be considerably lower in cv than in uv; moreover, quantitative addition of the re-established coat components to uv restored the high lipidic order.

Discussion

In the preceding section (Results) we have gathered potential arguments based on the behavior of TMA-DPH as an endocytic marker, for discriminating between the two models for the endocytic pathway. These include labeling features, kinetic data, and membrane fluidity evolution. This approach draws largely on the fact that TMA-DPH is principally transported across the endocytic pathway as a non-fluorescent solute and becomes fluorescent instantaneously in any membrane in contact with this solute, according to a partition equilibrium. This results in a correlation of the fluorescence intensity and the surface/volume ratio. In the following discussion, we present our reasons for thinking that the results do not conform to a vesicle-shuttle model, for the bulk transport at least, and then we examine how they match the maturation model.

The Vesicle-Shuttle or Pre-existing Compartments Model

In this model (Griffiths and Gruenberg, 1991) early and late endosomes pre-exist, independently of each other, as specific entities. Continuous transport between them is ensured by specific vesicular shuttle. A similar mechanism is probably assumed to be responsible for the transfer from late endosomes to lysosomes, although the authors say little about this. The actual TMA-DPH features and those predicted with this model are compared hereafter.

Labeling features. In a pulse-chase experiment, like that described in Fig. 1, *e* and *f*, TMA-DPH labeling is first observed (after 3 min of incubation) beneath the plasma membrane (early endosomal compartment) and after a 30-min chase it has moved inwards markedly with apparently the same brightness. This would not be possible with a vesicle shuttle mechanism. The shuttle movement being continuous, the ultimate situation would be balanced labeling of all compartments; the fluorescence would be observed over all regions of the cell with an equal, but reduced brightness.

Kinetic curves. TMA-DPH release curves (Fig. 3) give more insight than internalization curves. They describe the evolution of TMA-DPH fluorescence intensity after incubation with the probe followed by various chase times. Whatever the incubation time (even for 2 min) the curve presents, immediately after TAM-DPH chase, a very rapid decrease ($T_{1/2}$ 1.5 min). This decrease must be interpreted as resulting from direct exocytosis (reversible pinocytosis). Any other recycling process would be more delayed and slower. The second part of the curves is practically constant. No further significant decrease in fluorescence intensity is observed even 12 h after incubation. With a vesicle shuttle, the fluorescence intensity should continue to decrease in the second part of the curves, because of the decrease in the surface/volume ratio from early to late compartments. It is generally agreed the former are tubulo-vesicular in shape, while the latter are described as rather vesicular (see Courtoy, 1991, for a review). To our knowledge, no data on the size of endocytic compartments in L929 cells are available, but the study by Griffiths et al. (1989) on BHK cells should provide an order of magnitude. In these cells, the membrane area is 430 μm^2 and the volume 6.8 μm^3 in early endosomes, with 370 μm^2 and 36.8 μm^3 in the prelysosomal and lysosomal compartment. From these data it may be inferred, as regards to TMA-DPH labeling, that, at labeling equilibrium between the compartments, the fluorescence intensity should be 3.5 times lower than for the probe located only in the early compartment. This means that the progression in the endocytic pathway should be accompanied by a noticeable decrease in fluorescence intensity. Recycling is another reason why TMA-DPH fluorescence intensity should decrease. In the pre-existing compartments model, it is generally assumed that recycling occurs through individual vesicles budding off from endosomal tubular extensions so as to counter-balance the inverse flow of incoming endocytic vesicles. It has been shown clearly (Mayor et al., 1993) that the actual recycling mechanism is different and involves breaking away from important parts of endosomal tubular extensions. This mechanism is inconsistent per se with the preservation of specific compartments integrity. However, it is interesting to examine how recycling by individual vesicles might influence TMA-DPH fluorescence intensity. In the case of release kinetics, endocytic vesicles are unlabeled after TMA-DPH chase. Accordingly, considering a coupled fusion-recycling event occurring on a same labeled compartment, the only loss in fluorescence intensity would result from TMA-DPH dilution by 1-v/V (v and V respective volumes of vesicle and compartment). This is because the loss of surface due to recycling is compensated for by the fusing vesicle. With typical respective diameters of 50 and 500 nm (Courtoy, 1991), this means that such an event would reduce the fluorescence intensity by 1:1,000. Nevertheless, since the flow of endocytic vesicles is in the range of 10^3 min^{-1} (Griffiths and Gruenberg, 1991), this would rapidly result in a significant decrease in fluorescence intensity. Thus, the constant part of the kinetic release curves cannot be explained with this model.

Internalization kinetics, unlike release, could be interpreted a priori with the vesicle-shuttle model. The increase in intracellular fluorescence intensity resulting from the formation of endocytic vesicles is slowed down by reverse pinocytosis, recycling from endosomes (minor importance, see Fig. 2 *d*), and dilution during the transfer between compartments. These various contributions tend to a dynamic equilibrium consistent with the constant slope of the curve for long incubations. Nor are the curve trends inconsistent with the typical timing of the endocytic process in this model.

Fluorescence anisotropy data. Fluorescence anisotropy values of hydrophobic probes, such as TMA-DPH, account for the level of the lipidic order in membranes. This depends largely on the membrane phospholipidic composition and on cholesterol constant (Sawyer, 1988), and much less on the membrane composition in integral proteins (Devaux and Seigneuret, 1985). The results of the TMA-DPH pulse-chase experiment in L929 cells and mouse bone-marrow-derived macrophages (Fig. 4) have shown that, except for a very

early fluidity effect ($t_{1/2}$ 1 min) due to shedding of the clathrin coat by endocytic vesicles, TMA-DPH fluorescence intensity remains remarkably constant throughout the endocytic pathway. Moreover, its value is then exactly the same as in the bulk plasma membrane. In the pre-existing compartment model, each type of compartment is a specific organelle and should display a characteristic membrane fluidity level. This may, of course, vary considerably. For instance, with TMA-DPH, Mutet et al. (1984) report a fluorescence anisotropy of 0.210 in mitochondria, which is far from the values usually found in plasma membranes (0.285 and 0.272 in this study). Thus, transfer from early to late endosomes should be accompanied by a change in fluorescence anisotropy, which, however, is not observed. On the other hand, most authors agree that intracellular membranes are more fluid than the plasma membrane (see, for instance, Shinitzky and Barenholz, 1978; Gilmore et al., 1979; Kinosita et al., 1981; Whetton et al., 1983). Thus, finding the same membrane fluidity in endocytic compartment as in the plasma membrane is totally unexpected on the basis of a pre-existing compartments model. It should be noted, by the way, that this result provides further evidence that TMA-DPH is only internalized by endocytosis (non-existent as a cytosolic solute).

Finally, all these experimental aspects argue against a pre-existent compartments model for the bulk transport in the endocytic pathway. These data alone do not, of course, preclude, a priori, a low contribution of such a mechanism with a high specificity. Here, however, complementary information from other authors (Ward et al., 1989; Mayor et al., 1993) shows that specific ligands follow the bulk process at the same rate, and, thus, invalidates this assumption.

The Maturation Model

In this model (Murphy, 1991), endosomes are not independent pre-existing organelles. Early endosomes are formed by the coalescence of endocytic vesicles and are consumed by recycling events and by the generation of late endosomes. This presupposes the lipidic composition of all endocytic compartments to be the same, as had been observed by Belcher et al. (1987) in rat hepatocytes. Consequently, membrane fluidity should remain constant too, maintaining the same level as in the plasma membrane. Crossing with the secretory pathway from TGN should induce no significant modifications, as the corresponding flow is negligible compared to that of endocytosis (see Courtoy, 1991). The membrane protein composition does vary with maturation, but this should not influence the membrane fluidity either (Devaux and Seigneuret, 1985). These requirements are totally consistent with the evolution of TMA-DPH fluorescence anisotropy observed, which actually focused our attention on the maturation model.

From a kinetic point of view, any discussion on TMA-DPH release curves (Fig. 3) must consider carefully the recycling mechanism. Mayor et al. (1993) (see also Presley et al., 1993) unambiguously showed by quantitative fluorescence microscopy with the bulk membrane endocytic marker C_6-NBD-SM) that early endosomes release most of their membrane very rapidly ($t_{1/2}$ = 2.5 min). This was assumed to occur through large segments of endosomal tubular extensions immediately breaking off. These then concentrate in a pericentriolar recycling compartment, from where they recycle with a half-time of about 8 min. The remaining vesicular part of early endosomes, which makes up most of the volume but little surface, and contains most soluble ligands, is then available for further maturation and progression through the endocytic pathway. This might be a tempting mechanism to explain TMA-DPH release curves; the rapid initial decrease would correspond to intense recycling, and the constant part to fluorescence intensity stabilization in the remaining vesicular elements. However, this is hardly possible because the kinetics of the decreasing part of the curve are too rapid ($t_{1/2}$ 1.5 min) and the corresponding effect too early (very likely reverse pinocytosis). We hereafter propose an alternative development of the above mechanism which allows important and rapid recycling to be reconciled with constant intracellular TMA-DPH fluorescence intensity. Buddings of tubular elements from endosomes are considered as non-isolated independent events, but involved rather in a cascade process. Early endosomes have been described as discontinuous interacting networks (Hopkins et al., 1990; Tooze and Hollinshead, 1991). Tubular elements budding off from an endosome would fuse with another neighboring endosome and, in this way, trigger tubule budding from the latter, and so on. In the case of TMA-DPH release kinetics, labeled tubules breaking off would in this way be immediately replaced by unlabeled elements coming from newly formed endosomes, with no statistical change in surface due to recycling. The only change in fluorescence intensity would then result from dilution by the low-volume content of the unlabeled fusing tubule (see previous discussion on the pre-existing compartments model). This might correspond to a decrease of a few percent in fluorescence intensity, probably not detectable, but could become very important if the process were repeated many times. Here, however, contrary to the vesicle-shuttle model, this is a transient stage, and early endosomes rapidly ($t_{1/2}$ 3 min, based on the data of Schmid et al., 1988) escape to form late endosomes. We think that the way in which this occurs, without any decrease in TMA-DPH fluorescence intensity, is by the formation of multivesicular bodies. These structures have been described by many authors (Helenius et al., 1983; Hopkins, 1983; Wileman et al., 1985; Griffiths et al., 1988; Holtzman, 1989; Mc Dowell et al., 1989; Van Deurs et al., 1989; Burwen and Jones, 1991; Courtoy, 1991; Gorvel et al., 1991). They result from the pinching inwards of vesicles, to the detriment of the endosomal tubular element. The shape of endosomes becomes more vesicular and the budding tendency decreases, while motility is facilitated. This process results in no change in the surface/volume ratio, even though the overall shape is more spherical. Whether or not interendosomal fusions occur before or concomitantly has no importance in terms of fluorescence intensity, the surface/volume ratio being unchanged too. Such fusions are actually very likely to occur, since from Fig. 1, *c* and *d* it may be inferred that many of the compartments labeled with acridine orange are also labeled with TMA-DPH. This interpretation of the release cures emphasizes the complementarity of the information obtained with TMA-DPH. While TMA-DPH may be a poor marker for studying the recycling kinetics from endosomes, the mechanism described above for this recycling might not have been revealed with other bulk membrane markers. This interpretation is actually consistent with the other aspects of the behavior of TMA-DPH as an endocytic marker.

Labeling features, for instance, as in the pulse-chase experiment of Fig. 1, *e* and *f* fit with this model. After TMA-DPH has been chased, peripheral-labeled endosomes are progressively replaced by unlabeled endosomes (decrease in peripheral labeling), while the former move inwards (supposedly as multivesicular bodies) with no loss in intracellular fluorescence intensity, nor in apparent brightness.

TMA-DPH internalization curves (Fig. 3) are explained as follows. After the addition of TMA-DPH, labeled endocytic vesicles are formed, some of which recycle directly. The others fuse with each other to build endosomes, or fuse with previously formed unlabeled endosomes. These fusions induce no change in fluorescence intensity (surface/volume ratio is constant). While this process continues, tubules break off from the labeled endosomes formed, according to the cascade mechanism describe above, and fluorescence intensity is lost in recycling. An equilibrium between these events is rapidly reached (first part of the curve). The second part of the curve accounts then for those endosomes which, at a constant rate, escape from this equilibrium, by forming multivesicular bodies with constant fluorescence intensity (no more recycling). This second part of the curve is more affected than the first one by lowering the temperature, because prior formation of endosomes, involving fusions, is required. For the first part, even at low temperature, internalization, and direct recycling of endocytic vesicles would continue to occur.

Appendix

TMA-DPH partition equilibrium between membranes and aqueous media. The existence of the partition equilibrium was inferred from the proportionality of the TMA-DPH fluorescence intensity I_f to the cell (or membrane) concentration (Kuhry et al., 1985). In point of fact, the fluorescence intensity is proportional to the chromophore concentration in the sample, i.e., to the concentration of membranar TMA-DPH per unit volume of suspension.

$I_f = k[\text{TMA-DPH}]_{mb} V_{mb}/V_{aq}$ or
$I_f = k'[\text{TMA-DPH}]_{mb} N$
(V_{mb}, volume of membranes; v_{aq}, volume of buffer; N, cell density).

On the other hand, the partition equilibrium is written:

$[\text{TMA-DPH}]_{mb} = K[\text{TMA-DPH}]_{aq}$
(K, equilibrium constant) thus:
$I_f = K\,k'\,c\,(1\text{-}f)\,N$

The incorporated probe molar fraction f is low (typically 5%), so that I_f is approximately proportional to cell density and TMA-DPH total concentration, or, which amounts to the same, proportional to TMA-DPH concentration and membrane surface, the membrane thickness being constant.

The partition equilibrium is established instantaneously, which allows accurate monitoring of the rapid kinetics of stimulated exocytosis in various cell systems (Bronner et al., 1986; Kubina et al., 1987; Furuno et al., 1992; Heemskerk et al., 1993). The partition equilibrium constant K varies little from one biological membrane to another (see text, section Results), so that TMA-DPH fluorescence intensity measurements may be used for cell surface evaluation (Siffert et al., 1993).

This partition property has been compared to that of other diphenylhexatriene derivatives by Huang and Haugland (1991).

It should be noted, that, with the maturation model, the constant K must, in theory, be identical in all endocytic compartments (the incorporation is determined by the lipid but not by the protein membrane composition).

Received for publication 23 July 1993 and in revised form 1 February 1994.

References

Anderson, R. G. W. 1993. Dissecting clathrin-coated pits. *Trends Cell Biol.* 3:177–179.

Anderson, R. G. W., and L. Orci. 1988. A view of acidic intracellular compartments. *J. Cell Biol.* 106:539–543.

Beaumelle, B. D., A. Gibson, and C. R. Hopkins. 1990. Isolation and preliminary characterization of the major membrane boundaries of the endocytic pathway in lymphocytes. *J. Cell Biol.* 111:1811–1823.

Belcher, J. D., R. L. Hamilton, S. E. Brady, C. A. Hornick, S. Haeckle, W. J., and R. J. Havel. 1987. Isolation and characterization of three endosomal fractions from the liver of estradiol-treated rats. *Proc. Natl. Acad. Sci. USA.* 84:6785–6789.

Berlin, R. D., and J. M. Oliver. 1980. Surface functions during mitosis. *J. Cell Biol.* 85:660–671.

Besterman, J. M., J. A. Airhart, R. C. Woodworth, and R. B. Low. 1981. Exocytosis of pinocytosed fluid in cultured cells: kinetic evidence for rapid turnover and compartmentation. *J. Cell Biol.* 91:716–727.

Bomsel, M., R. Parton, S. A. Kuznetsov, T. A. Schroer, and J. Gruenberg. 1990. Microtubule- and motor-dependent fusion *in vitro* between apical and basolateral endocytic vesicles from MDCK cells. *Cell.* 62:719–731.

Brodsky, F. M. 1988. Living with clathrin: its role in intracellular membrane traffic. *Science (Wash. DC).* 242:1396–1402.

Brodsky, F. M., B. L. Hill, S. L. Acton, I. Näthke, D. H. Wong, S. Ponnambalam, and P. Parham. 1991. Clathrin light chains: arrays of protein motifs that regulate coated-vesicle dynamics. *Trends Biochem. Sci.* 16:209–213.

Bronner, C., Y. Landry, P. Fonteneau, and J. G. Kuhry. 1986. Fluorescent hydrophobic probe used for monitoring the kinetics of exocytosis phenomena. *Biochemistry.* 25:2149–2154.

Burwen, S. J., and A. L. Jones. 1991. Intracellular pathways of immunoglobulin A and epidermal growth factor transport in hepatocytes. *In* Intracellular Trafficking of Proteins. C. J. Steer, A. Hanover, editors. Cambridge University Press, Cambridge, New York, Port-Chester, Melbourne, Sydney. 248–278.

Courtoy, P. J. 1991. Dissection of endosomes. *In* Intracellular Trafficking of Proteins. C. J. Steer and A. Hanover, editors. Cambridge University Press, Cambridge, New York, Port Chester, Melbourne, Sydney. 104–155.

Cranney, M., R. B. Cundall, G. R. Jones, J. T. Richard, and E. W. Thomas. 1983. Fluorescence lifetime and quenching studies on some interesting diphenylhexatriene probes. *Biochim. Biophys. Acta.* 735:418–425.

Daukas, G., D. A. Lauffenburger, and S. I. Zigmond. 1983. Reversible pinocytosis in polymorphonuclear leukocytes. *J. Cell Biol.* 96:1642–1650.

Devaux, P., and M. Seigneuret. 1985. Specificity of lipid-protein interactions as determined by spectroscopic techniques. *Biochim. Biophys. Acta.* 822: 63–125.

Dunn, K. W., and F. R. Maxfield. 1992. Delivery of ligands from sorting endosomes to late endosomes occurs by maturation of sorting endosomes. *J. Cell Biol.* 117:301–310.

Dunn, W. A., A. L. Hubbard, and N. N. Aronson, Jr. 1980. Low temperature selectively inhibits fusion between pinocytic vesicles and lysosomes during heterophagy of ^{125}I-asialofetuin by the perfused rat liver. *J. Biol. Chem.* 255:5971–5978.

Dunn, W. A., T. P. Connolly, and A. L. Hubbard. 1986. Receptor-mediated endocytosis of epidermal growth factor by rat hepatocytes: receptor pathway. *J. Cell Biol.* 102:24–36.

Duportail, G., and A. Weinreb. 1983. Photochemical changes of fluorescent probes in membranes and their effect on the observed fluorescence anisotropy values. *Biochim. Biophys. Acta.* 736:171–177.

Feng, Y., and M. Forgac. 1992. A novel mechanism for regulation of vacuolar acidification. *J. Biol. Chem.* 367:19769–19772.

Furuno, T., R. Isoda, K. Inagaki, T. Iwaki, M. Noji, and M. Nakanishi. 1992. A fluorescent molecular rotor probes the kinetic process of degranulation of mast cells. *Immunol. Lett.* 33:285–288.

Geuze, H. J., W. Stoorvogel, G. J. Strous, J. W. Slot, J. E. Bleekemolen, and I. Mellman. 1988. Sorting of mannose 6-phosphate receptors and lysosomal membrane proteins in endocytic vesicles. *J. Cell Biol.* 107:2491–2501.

Gilmore, R., N. Cohn, and M. Glaser. 1979. Rotational relaxation times of 1,6-diphenyl-1,3,5-hexatriene in phospholipids isolated from LM cell membranes. Effect of polar head-group and fatty acid composition. *Biochemistry.* 18:1050–1056.

Goldstein, J. L., M. S. Brown, R. G. W. Anderson, D. W. Russel, and W. J. Schneider. 1985. Receptor-mediated endocytosis: concepts emerging from LDL. *Annu. Rev. Cell Biol.* 1:1–39.

Gorvel, J. P., P. Chavrier, H. Zerial, and J. Gruenberg. 1991. Rab 5 controls early endosome fusion *in vitro*. *Cell.* 64:915–925.

Goud, B., C. Jouanne, and J. C. Antoine. 1984. Reversible pinocytosis of horseradish peroxidase in lymphoid cells. *Exp. Cell Res.* 153:218–235.

Griffiths, G., and J. Gruenberg. 1991. The arguments for pre-existing early and late endosomes. *Trends Cell Biol.* 1:5–9.

Griffiths, G., R. Back, and M. Marsh. 1989. A quantitative analysis of the endocytic pathway in baby hamster kidney cells. *J. Cell Biol.* 109:2703–2720.

Griffiths, G., R. Matteoni, R. Back, and B. Hoflack. 1990. Characterization of the cation-independent mannose-6-phosphate receptor-enriched prelysosomal compartment in NRK cells. *J. Cell Sci.* 95:441–461.

Grinnell, F. 1978. Cellular adhesiveness and extracellular substrate. *Int. Rev. Cytol.* 53:65–144.

Gruenberg, J., and K. E. Howell. 1989. Membrane traffic in endocytosis: insights from cell-free assays. *Annu. Rev. Cell Biol.* 5:453–481.

Gruenberg, J., G. Griffiths, and K. E. Howell. 1989. Characterization of the early endosome and putative endocytic carrier vesicles in vivo and with an assay of vesicle fusion in vitro. *J. Cell Biol.* 108:1301–1316.

Hare, J. F. 1988. Dissection of membrane protein degradation mechanisms by reversible inhibitors. *J. Biol. Chem.* 263:8759–8764.

Haugland, R. P. 1992. Molecular probes. Handbook of fluorescent probes and research chemicals. Molecular Probes Inc., Eugene, OR. 260–266.

Haylett, T., and L. Thilo. 1991. Endosome-lysosome fusion at low temperature. *J. Biol. Chem.* 266:8322–8327.

Heemskerk, J. W. M., M. A. H. Feijge, J. A. M. Andree, and S. O. Sage. 1993. Function of intracellular $[Ca^{2+}]_i$ in exocytosis and transbilayer movement in human platelets surface-labeled with the fluorescence probe 1-(4-trimethylammonium)phenyl)-6-phenyl-1,3,5-hexatriene. *Biochim. Biophys. Acta.* 1147:194–204.

Helenius, A., I. Mellman, D. Wall, and A. Hubbard. 1983. Endosomes. *Trends Biochem. Sci.* 8:245–249.

Heuser, J. 1989. Changes in lysosome shape and distribution correlated with changes in cytoplasmic pH. *J. Cell Biol.* 108:855–864.

Holtzman, E. 1989. Lysosomes. Chapter 3. Acidification; membrane properties; permeability and transport. Plenum Press, New York. 93–139.

Hopkins, C. R. 1983. The importance of endosomes in intracellular traffic. *Nature (Lond.).* 304:684–685.

Hopkins, C. R., A. Gibson, M. Shipman, and K. Miller. 1990. Movement of internalized ligand-receptor complexes along a continuous endosomal reticulum. *Nature (Lond.).* 346:335–339.

Huang, Z., and R. P. Haugland. 1991. Partition coefficients of fluorescent probes with phospholipid membranes. *Biochem. Biophys. Res. Commun.* 181:166–171.

Hubbard, A. L. 1989. Endocytosis. *Curr. Opin. Cell Biol.* 1:675–683.

Illinger, D., P. Poindron, P. Fonteneau, M. Modollel, and J. G. Kuhry. 1990*a*. Internalization of the lipophilic fluorescent probe trimethylamino-diphenylhexatriene follows the endocytosis and recycling of the plasma membrane in cells. *Biochim. Biophys. Acta.* 1030:73–81.

Illinger, D., P. Poindron, N. Glasser, M. Modollel, and J. G. Kuhry. 1990*b*. The plasma-membrane internalization and recycling is enhanced in macrophages upon activation with gamma-interferon and lipopolysaccharide, a study using the fluorescent probe trimethylaminodiphenylhexatriene. *Biochim. Biophys. Acta.* 1030:82–87.

Illinger, D., P. Poindron, and J. G. Kuhry. 1991. Fluid phase endocytosis investigated by fluorescence with trimethylamino-diphenylhexatriene in L929 cells; the influence of temperature and of cytoskeleton depolymerizing drugs. *Biol. Cell.* 73:131–138.

Illinger, D., L. Italiano, J. P. Beck, C. Waltzinger, and J. G. Kuhry. 1994. Comparative evolution of endocytosis levels and or the cell surface area during the L929 cell cycle; a fluorescence study with TMA-DPH. *Biol. Cell.* In press.

Keen, J. H. 1990. Clathrin and associated assembly and disassembly proteins. *Annu. Rev. Biochem.* 59:415–438.

Kinosita, K., Jr., R. Kataoka, Y. Kimura, O. Gotoh, and A. Ikegami. 1981. Dynamic structure of biological membranes as probed by 1,6-diphenyl-1,3,5-hexatriene: a nanosecond fluorescence depolarization study. *Biochemistry.* 20:4270–4277.

Kinosita, K., S. Kawato, and A. Ikegami. 1977. A theory of fluorescence polarization decay in membranes. *Biophys. J.* 37:461–464.

Kok, J. W., M. ter Beest, G. Scherphof, and D. Hoekstra. 1990. A non exchangeable fluorescent phospholipid analog as a membrane traffic marker of the endocytic pathway. *Eur. J. Cell Biol.* 53:173–184.

Kornfeld, S., and I. Mellman. 1989. The biogenesis of lysosomes. *Annu. Rev. Cell. Biol.* 5:483–525.

Koval, M., and R. E. Pagano. 1989. Lipid recycling between the plasma membrane and intracellular compartments: transport and metabolism of fluorescent sphingomyelin analogues in cultured fibroblasts. *J. Cell Biol.* 108: 2169–2181.

Kubina, M., F. Lanza, J. P. Cazenave, G. Laustriat, and J. G. Kuhry. 1987. Parallel investigation of exocytosis and membrane fluidity changes in human platelets with the fluorescent probe TMA-DPH. *Biochim. Biophys. Acta.* 901:138–146.

Kuhry, J. G., P. Fonteneau, G. Duportail, C. Maechling, and G. Laustriat. 1983. TMA-DPH: a suitable fluorescence polarization probe for specific plasma membrane fluidity studies in intact living cells. *Cell Biophys.* 5:129–140.

Kuhry, J. G., G. Duportail, C. Bronner, and G. Laustriat. 1985. Plasma membrane fluidity measurements on whole living cells by fluorescence anisotropy of trimethylamino-diphenylhexatriene. *Biochim. Biophys. Acta.* 845:60–67.

Marsh, M., G. Griffiths, G. E. Dean, I. Mellman, and A. Helenius. 1986. Three-dimensional structure of endosomes in BHK-21 cells. *Proc. Natl. Acad. Sci. USA.* 83:2899–2903.

Mayor, S., J. F. Presley, and F. R. Maxfield. 1993. Sorting of membrane components from endosomes and subsequent recycling to the cell surface occurs by a bulk flow process. *J. Cell Biol.* 212:1257–1269.

Mayorga, L. S., R. Diaz, and P. D. Stahl. 1989. Regulatory role for GTP-binding proteins in endocytosis. *Science (Wash. DC).* 244:1475–1477.

McDowall, A., J. Gruenberg, K. Römisch, and G. Griffiths. 1989. The structure of organelles of the endocytic pathway in hydrated cryosections of cultured cells. *Eur. J. Cell Biol.* 49:281–294.

Mellman, I., R. Fuchs, and A. Helenius. 1986. Acidification of the endocytic and exocytic pathways. *Annu. Rev. Biochem.* 55:663–700.

Méresse, S., and B. Hoflack. 1993. Phosphorylation of the cation-independent mannose 6-phosphate receptor is closely associated with its exit from the *trans*-Golgi network. *J. Cell Biol.* 120:67–75.

Murphy, R. F. 1988. Processing of endocytosed material. *Adv. Cell Biol.* 2:159–180.

Murphy, R. F. 1991. Maturation models for endosomes and lysosome biogenesis. *Trends Cell Biol.* 1:77–82.

Mutet, C., G. Duportail, G. Cremel, and A. Waksman. 1984. Increase of the fluidity of the lipid bilayer of the inner mitochondrial membrane by succinate and phenyl-succinate: a study by EPR and fluorescence. *Biochem. Biophys. Res. Comm.* 119:854–859.

Paddenberg, R., C. Wiegand, and B. M. Jockusch. 1990. Characterization of the coated vesicle uncoating ATPase: tissue distribution, association with and activity on intact coated vesicles. *Eur. J. Cell Biol.* 52:60–66.

Padh, H., J. Ha, M. Lavassa, and T. Steck. 1993. A post lysosomal compartment in *Dictyostelium discoideum*. *J. Biol. Chem.* 268:6742–6747.

Pearse, B. M. F., and M. S. Bretscher. 1981. Membrane recycling by coated vesicles. *Annu. Rev. Biochem.* 50:85–101.

Pearse, B. M. F., and M. S. Robinson. 1990. Clathrin, adaptors, and sorting. *Annu. Rev. Cell. Biol.* 6:151–171.

Poujet, J., J. Munier, and B. Valeur. 1989. Correction of systematic phase errors in frequency-domain fluorometry. *J. Phys. E. Sci. Instrum.* 22:855–862.

Prendergast, F. G., R. P. Haugland, and P. J. Callahan. 1981. 1-[4-(trimethylamino)phenyl]-6-phenylhexa-1,3,5-triene: synthesis, fluorescence properties and use as a fluorescent probe of lipid bilayers. *Biochemistry.* 20:7333–7338.

Presley, J. F., S. M. Mayor, K. W. Dunn, L. S. Johnson, T. E. McGraw, and F. R. Maxfield. 1993. The *End 2* mutation in CHO cells slows the exit of transferrin receptors from the recycling compartment but bulk membrane recycling is unaffected. *J. Cell Biol.* 122:1231–1241.

Roederer, M., R. Bowser, and R. F. Murphy. 1987. Kinetics and temperature dependence of exposure of endocytosed material to proteolytic enzymes and low pH: evidence for a maturation model for the formation of lysosomes. *J. Cell Physiol.* 131:200–209.

Roederer, M., J. R. Barry, R. B. Wilson, and R. F. Murphy. 1990. Endosomes can undergo an ATP-dependent density increase in the absence of dense lysosomes. *Eur. J. Cell. Biol.* 51:229–234.

Rolland, J. M., G. R. Ferrier, R. C. Nairn, and M. N. Cauchi. 1976. Acridine orange fluorescence cytochemistry for detecting lymphocyte immunoreactivity. *J. Immunol. Meth.* 12:347–354.

Salzman, N. H., and F. R. Maxfield. 1988. Intracellular fusion of sequentially formed endocytic compartments. *J. Cell Biol.* 106:1083–1091.

Sandvig, K., and B. Van Deurs. 1990. Selective modulation of the endocytic uptake of ricin and fluid phase markers without alteration in transferrin endocytosis. *J. Biol. Chem.* 265:6382–6388.

Sawyer, W. H. 1988. Fluorescence spectroscopy in the study of membrane fluidity: model membrane systems. *In* Methods for Studying Membrane Fluidity. C. R. Aloia, C. C. Curtain, and L. M. Gordon, editors. Alan R. Liss Press, New York. 161–191.

Schmid, S. L. 1993. Coated-vesicle formation *in vitro*: conflicting result using different assays. *Trends Cell Biol.* 3:145–148.

Schmid, S. L., R. Fuchs, P. Male, and I. Mellman. 1988. Two distinct subpopulations of endosomes involved in membrane recycling and transport to lysosomes. *Cell.* 52:73–83.

Shinitzky, M., and Y. Barenholz. 1978. Fluidity parameters of lipid regions determined by fluorescence polarization. *Biochim. Biophys. Acta.* 515:367–394.

Siffert, J. C., O. Baldacini, J. G. Kuhry, D. Wacksmann, S. Benabdelmoumene, A. Faradji, H. Monteil, and P. Poindron. 1993. Effects of *Clostridium difficile* toxin B on human monocytes and macrophages: possible relationship with cytoskeletal rearrangement. *Infect. Immun.* 61:1082–1090.

Smythe, E., and G. Warren. 1991. The mechanism of receptor-mediated en-

docytosis. *Eur. J. Biochem.* 202:689–699.
Steer, C. J., and J. A. Hanover. 1991. Intracellular trafficking of proteins. Cambridge University Press, Cambridge, New York, Port Chester, Melbourne, Sydney. 1–348.
Steinman, R. M., I. S. Mellman, W. A. Muller, and Z. A. Cohn. 1983. Endocytosis and the recycling of plasma membrane. *J. Cell Biol.* 96:1–27.
Stoorvogel, W., G. J. Strous, H. J. Geuze, V. Oorschot, and A. L. Schwartz. 1991. Late endosomes derive from early endosomes by maturation. *Cell.* 65:417–427.
Storrie, B., R. R. Pool, Jr., M. Sachdeva, K. M. Maurey, and C. Oliver. 1984. Evidence for both prelysosomal and lysosomal intermediate in endocytic pathways. *J. Cell Biol.* 98:108–115.
Swanson, J., E. Burke, and S. C. Silverstein. 1987. Tubular lysosomes accompanying stimulated pinocytosis in macrophages. *J. Cell Biol.* 104:1217–1222.
Thilo, L. 1985. Quantification of endocytosis-derived membrane traffic. *Biochim. Biophys. Acta.* 822:243–266.
Tooze, J., and M. Hollinshead. 1991. Tubular early endosomal networks in AtT 20 and other cells. *J. Cell Biol.* 115:635–653.
Tuomikoski, T., M. A. Felix, M. Dorée, and J. Gruenberg. 1989. Inhibition of endocytic vesicle fusion *in vitro* the cell-cycle control protein kinase cdc 2. *Nature (Lond.).* 342:942–945.
Van Blitterswijk, W. J., R. P. Van Hoeven, and B. W. Van Der Meer. 1981. Lipid structural order parameters (reciprocal of fluidity) in biomembranes derived from steady-state fluorescence polarization measurements. *Biochim. Biophys. Acta.* 644:323–332.
Van Deurs, B., O. W. Petersen, S. Olsnes, and K. Sandvig. 1989. The ways of endocytosis. *Int. Rev. Cytol.* 117:131–177.
Von Figura, K. 1991. Molecular recognition and targeting of lysosomal proteins. *Curr. Biol.* 3:642–646.
Wang, L. H., K. G. Rothberg, and R. G. W. Anderson. 1993. Mis-assembly of clathrin lattices on endosomes reveals a regulatory switch for coated pit formation. *J. Cell Biol.* 123:1107–1117.
Ward, D. M., R. Ajioka, and J. Kaplan. 1989. Cohort movement of different ligands and receptors in intracellular endocytic pathway of alveolar macrophages. *J. Biol. Chem.* 264:8164–8170.
Ward, D. H., D. P. Hackenyos, and J. Kaplan. 1990. Fusion of sequentially internalized vesicles in alveolar macrophages. *J. Cell Biol.* 110:1013–1022.
Wessling-Resnick, M., and W. A. Braell. 1990. Characterization of the mechanism of endocytic vesicle fusion *in vitro*. *J. Biol. Chem.* 265:16751–16759.
Whetton, A. D., M. D. Houslay, N. J. F. Dodd, and W. H. Evans. 1983. The lipid fluidity of rat liver membrane subfractions. *Biochem. J.* 214:851–854.
Wileman, T., C. Harding, and P. Stahl. 1985. Receptor mediated endocytosis. *Biochem. J.* 232:1–14.
Wilson, D. W., S. W. Whiteheart, L. Orci, and J. E. Rothman. 1991. Intracellular membrane fusion. *Trends Biochem. Sci.* 16:334–337.
Wu, J. R., and B. R. Lentz. 1991. Mechanisms of polyethylene glycol induced lipid transfer between phosphatidylcholine large unilamellar vesicles: a fluorescent probe study. *Biochemistry.* 30:6780–6787.
Yamashiro, D. J., and F. R. Maxfield. 1988. Regulation of endocytic processes by pH. *Trends Pharmacol. Sci.* 9:190–193.